

DOI: 10.31319/2519-8106.1(52)2025.330532  
UDC 669.018.5:541.128:536.7

**Belokon Yuriy**<sup>1</sup>, Doctor of Technical Sciences, Professor, Head of Department of Metallurgical Technologies, Ecology and Technological Safety

**Бєлоконь Ю.О.**, доктор технічних наук, професор, завідувач кафедри металургійних технологій, екології та техногенної безпеки

ORCID: 0000-0002-9327-5219

e-mail: belokon.zp@gmail.com

**Zholobko Bohdan**<sup>1</sup>, Postgraduate student, Junior Scientific Assistant, Assistant of Department of Metallurgical Technologies, Ecology and Technological Safety

**Жолобко Б.О.**, здобувач третього (доктор філософії) рівня вищої освіти, молодший науковий співробітник, асистент кафедри металургійних технологій, екології та техногенної безпеки

ORCID: 0009-0005-5567-0743

e-mail: zholobko.ph@znu.edu.ua

**Sahuliakin Oleksandr**<sup>1</sup>, Postgraduate student, Junior Scientific Assistant, Assistant of Department of Metallurgical Technologies, Ecology and Technological Safety

**Сагулякін О.Є.**, здобувач третього (доктора філософії) рівня вищої освіти, молодший науковий співробітник, асистент кафедри металургійних технологій, екології та техногенної безпеки

ORCID: 0009-0009-9153-2806

e-mail: aleksandrsagulakin@gmail.com

**Sereda Dmytro**<sup>2</sup>, Candidate of Technical Sciences, Associate Professor, Department of industrial engineering

**Серєда Д.Б.**, кандидат технічних наук, доцент кафедри галузевого машинобудування господарство

ORCID: 0000-0003-4353-1365

e-mail: seredabp@ukr.net

**Yavtushenko Anna**<sup>1</sup>, Candidate of Technical Sciences, Associate Professor of Department of Metallurgical Technologies, Ecology and Technological Safety

**Явтушенко А.В.**, кандидат технічних наук, доцент кафедри металургійних технологій, екології та техногенної безпеки

ORCID: 0000-0003-1112-5426

e-mail: yavtushenko.anna.v@gmail.com

<sup>1</sup>Zaporizhzhia National University, Zaporizhzhia

Запорізький національний університет, Запоріжжя

<sup>2</sup>Dniprovsky State Technical University, Kamianske

Дніпровський державний технічний університет, Кам'янське

## DESIGN AND THERMODYNAMIC EVALUATION OF A MULTI-COMPONENT HIGH ENTROPY ALLOY CATALYST Al-Ni-Co-Fe-Cu-Mn UNDER THERMOCHEMICAL PRESSING CONDITIONS

### РОЗРОБКА ТА ТЕРМОДИНАМІЧНА ОЦІНКА БАГАТОКОМПОНЕНТНОГО ВИСОКОЕНТРОПНОГО СПЛАВНОГО КАТАЛІЗАТОРА Al-Ni-Co-Fe-Cu-Mn В УМОВАХ ТЕРМОХІМІЧНОГО ПРЕССУВАННЯ

*High-entropy alloys (HEAs) are multicomponent materials containing five or more elements in near-equiatomic or carefully selected ratios. Using high configurational entropy, HEAs stabilize simple crystal structures such as face-centered cubic (FCC) or volume-centered cubic (VCC), which provides*

*exceptional properties: high mechanical strength, resistance to oxidation at high temperatures, and natural catalytic potential. These qualities make WEC ideal for innovative applications. The compositional flexibility of systems such as Al-Ni-Co-Fe-Cu-Mn allows for fine-tuning of microstructure and surface characteristics, contributing to the creation of stable active centers under thermochemical conditions. Existing research in the field of materials science confirms their superiority over traditional materials.*

**Keywords:** *high-entropy alloys, configurational entropy, crystal structures, catalytic potential, thermochemical resilience, Al-Ni-Co-Fe-Cu-Mn.*

*Високоентропійні сплави (ВЕС) це багатокомпонентні матеріали, що містять п'ять або більше елементів у близьких до еквіатомних чи ретельно підібраних співвідношеннях. Використовуючи високу конфігураційну ентропію, ВЕС стабілізують прості кристалічні структури, такі як гранецентрована кубічна (ГЦК) або об'ємноцентрована кубічна (ОЦК), що забезпечує виняткові властивості: високу механічну міцність, стійкість до окислення при високих температурах і природний каталітичний потенціал. Ці якості роблять ВЕС ідеальними для інноваційних застосувань. Композиційна гнучкість систем, таких як Al-Ni-Co-Fe-Cu-Mn, дозволяє точно налаштовувати мікроструктуру та поверхневі характеристики, сприяючи створенню стійких активних центрів у термохімічних умовах. Наявні дослідження у області матеріалознавства, підтверджують їх перевагу над традиційними матеріалами. Це дослідження зосереджене на розробці та термодинамічній оцінці ВЕС з метою використання у процесах каталітичного відновлення газових фаз. Мета розвитку каталітичних матеріалів у напрямку ВЕС супроводжується необхідністю отримання альтернативи наявним високовартісним платиновим каталізаторам. У дослідженні розглядаються 4 системи різного складу, та порівнюються їх термодинамічні властивості.*

**Ключові слова:** *високоентропійні сплави, конфігураційна ентропія, кристалічні структури, каталітичний потенціал, термохімічна стійкість, Al-Ni-Co-Fe-Cu-Mn.*

### Problem's Formulation

High-entropy alloys (HEA) are materials that have unique physical and chemical parameters due to the richness of the systems, so their research and development are important for further progress. The high configuration entropy of rich component systems with a strong warehouse ensures the formation of a stable crystal lattice such as BCC or FCC, which increases mechanical strength, resistance to oxidation for high temperatures and potency of formation of active catalytic centers. The main goal of this research lies in the development of a system of non-equiatomic high-entropy alloy for thermochemical presing using methods of mathematical modeling of synthesis and assessment of physicochemical and thermodynamic parameters for vicorization in catalyst components in thermochemical processes at high temperatures. The main focus of this achievement is on the selection of the optimal molar ratio of elements to achieve optimal parameters of thermodynamic reactions, ensured phase stability and proximity to ideal dissolution.

### Analysis of recent research and publications

Research on high-entropy alloys describes their potential as catalysts due to their multi-element composition, which leads to high configurational entropy and structural stability. The main focus is on studying their thermodynamic properties and catalytic performance in various applications, including gas purification.

In general, the HES effect is achieved through the interaction between elements, which affects catalytic activity and stability. Pt-containing HESs demonstrate high activity in HER and MOR due to multiple active sites and fast electron transfer [3]. Platinum-free catalysts such as CoFeNiGaZn achieve 98 % conversion of CO to CO<sub>2</sub> at 500 °C, which is explained by the transfer of electrons from nickel to adsorbed CO and O<sub>2</sub> molecules [1]. The CoNiCuRuPd system in the form of a surface layer based on TiO<sub>2</sub> demonstrates high activity in the hydrogenation of CO<sub>2</sub> with a CH<sub>4</sub> selectivity of 68.3 % at 400 °C, which is associated with the release of hydrogen [2]. Thus, WPPs as a class can carry out CO oxidation and related reactions involving CO, VOCs and H<sub>2</sub>S.

To design a catalyst, a necessary step is to determine the general thermodynamic properties. The method of calculating the enthalpy of mixing is to use the Miedema model; the result of the calculations

should be enthalpy values from -22 to 7 kJ/mol, which contribute to the formation of a solid solution. For HEA,  $\Delta S_{mix} > 1.5R$  (approximately 12.47 J/(mol·K)) stabilises disordered phases [6].

Coke gas purification requires catalysts capable of handling the complex gas composition (55—60 %  $H_2$ , 23—27 %  $CH_4$ , 5—8 %  $CO$ , 1.5—3 %  $CO_2$ , 2—4 %  $C_nH_m$ ) and meeting strict standards (e.g. sulphur  $\leq 0.1$  mg/nm<sup>3</sup>, phenols  $\leq 1$  mg/nm<sup>3</sup>) [7]. Current research on HEA catalysts for high-temperature processes with gaseous phases is limited, especially for *Mn*-containing alloys. Main function of *Mn* is improving redox properties, as in the case of nanoporous HEAs for CO oxidation [8]. However, there is a lack of data on Al-Ni-Co-Fe-Cu-Mn systems at 900—1300 °C, but there are calculations of the reduction intensity for intermetallic systems [9]. For example, *PtPdCoNiMn* shows high activity in oxygen reduction [4], but there is a lack of high-temperature tests relevant to coke production and the general type of platinum catalysts is the opposite direction of development from this study.

Empirical and semi-empirical methods, such as the CALPHAD method and first-principles calculations, are used to obtain data on the stability of HEAs [6]. HEA with moderate  $\Delta H_{mix}$  and high  $\Delta S_{mix}$  are resistant to phase decomposition. However, the use of non-equimolar compositions, such as *Al<sub>25</sub>Ni<sub>15</sub>Co<sub>15</sub>Fe<sub>15</sub>Cu<sub>15</sub>Mn<sub>15</sub>*, has not been sufficiently studied, and there is a lack of information on the use and optimisation of HEA composition for high-temperature gas cleaning. It should be noted that the lack of experimental data on the role of *Mn* at 900—1300 °C limits the understanding of its contribution to the conversion of *CO* and *H<sub>2</sub>S*.

### Formulation of the study purpose

The purpose of this study is to develop and preliminary thermodynamically evaluate a highly entropy system of Al-Ni-Co-Fe-Cu-Mn with different molar configurations of molar composition, which aims to create a catalytic highly entropy alloy for gas phase purification. The main task is mathematical modeling and calculation of key parameters of the formation of a highly entropic alloy such as enthalpy —  $\Delta H_{mix}$  and entropy —  $\Delta S_{mix}$  mixing, free Gibbs energy —  $\Delta G_{mix}$  to assess phase stability and catalysis ability in the temperature range 900—1300 °C. The Miedema model for binary compounds and their interaction is used as the main one for calculations.

### Presenting main material

For the thermodynamic analysis of the properties of high-entropy alloys, the following formulas were used:

$$\Delta S_{mix} = -R \sum_{i=1}^n c_i \cdot \ln c_i, \quad (1)$$

where:  $R$  — the universal gas constant,  $R=8.314$  J/(mol·K);  $\sum = \ln c_i$  — summation from  $i=1$  to, where  $n$  is the number of components in the alloy;  $c_i$  — the molar fraction of the  $i$ -th component in the alloy.

$\ln c_i$  — the natural logarithm of the molar fraction of the  $i$ -th component.

$$\Delta H_{mix} = 4 \sum_{i=1}^4 \sum_{j=i+1}^5 c_i c_j H_{ij}, \quad (2)$$

where:  $c_i$  is molar fraction of the  $i$ -th component;  $c_j$  is molar fraction of the  $j$ -th component;  $H_{ij}$  is mixing enthalpy between the  $i$ -th and  $j$ -th components, measured in kJ/mol.

$$\Delta G_{mix} = \Delta H_{mix} - T \cdot \Delta S_{mix}, \quad (3)$$

where:  $\Delta G_{mix}$  — the Gibbs free energy of mixing (measured in kJ/mol);  $\Delta H_{mix}$  — the mixing enthalpy (from Formula 2);  $T$  — the temperature (measured in Kelvin, e.g.,  $T=298$  K for room temperature);  $\Delta S_{mix}$  — the mixing entropy (from Formula 1)

$$VEC_{HEA} = \sum_{i=1}^n c_i (VEC)_i, \quad (4)$$

where:  $c_i$  — the molar fraction of the  $i$ -th component;  $(VEC)_i$  — the valence electron concentration of the  $i$ -th component (number of valence electrons).

These formulas enabled the evaluation of key alloy parameters that influence its phase stability and crystalline structure. Specifically,  $\Delta S_{mix}$  reflects the degree of disorder in the system, a defining characteristic of high-entropy alloys.  $\Delta H_{mix}$ , which depends on pairwise elemental interactions, aids in assessing the energetic contribution to alloy formation, though accurate values require experimental  $H_{ij}$  data.  $\Delta G_{mix}$  integrates entropic and enthalpic contributions, facilitating predictions of phase

thermodynamic stability at a given temperature [5]. Finally, the valence electron concentration ( $VEC_{HEA}$ ) indicates the potential coexistence of FCC and BCC phases, but in this study, we focused on modeling both structures separately to gain deeper insight into their individual contributions [6].

Table 1.  $\Delta H_{mix}$  calculated for binary systems using the Miedema model

—	Al	Ni	Co	Fe	Cu	Mn
Al	—	-22	-19	-11	-7,6	-19
Ni	-22	—	-9	-2	3,6	-8
Co	-19	-9	—	-1	6	-5
Fe	-11	-2	-1	—	13	5
Cu	-7,6	3,6	6	13	—	4
Mn	-19	-8	-5	-5	4	—

Four alloys were selected for the calculation of the required high-entropy system intended for use in catalytic processes:

- Al<sub>20</sub>Ni<sub>20</sub>Co<sub>20</sub>Fe<sub>20</sub>Cu<sub>20</sub>
- Al<sub>28</sub>Ni<sub>22</sub>Co<sub>17</sub>Fe<sub>15</sub>Cu<sub>10</sub>Mn<sub>8</sub>
- Al<sub>32</sub>Mn<sub>23</sub>Ni<sub>17</sub>Fe<sub>8</sub>Cu<sub>8</sub>Co<sub>12</sub>
- Al<sub>32</sub>Ni<sub>15</sub>Co<sub>13</sub>Mn<sub>15</sub>Fe<sub>10</sub>Cu<sub>15</sub>

One of the primary conditions for achieving a solid solution in a high-entropy system is adherence to the following condition:

$$13,4 \leq \Delta S_{mix} \leq 22 \left( \frac{J}{mol \cdot K} \right). \quad (5)$$

Based on data obtained from open sources, mathematical modeling of several systems with varying molar configurations was conducted. This was done to determine the optimal composition of a high-entropy alloy (HEA) that would meet the specified parameters required for synthesis and subsequent performance as a catalytic product. For the synthesis of the HEA, the Al-Ni-Co-Fe-Cu-Mn system was selected. A detailed analysis of this system necessitates an explanation of the choice of specific elements.

The foundation of the HEA is aluminum, which promotes the formation of the BCC phase due to its low valence electron concentration ( $VEC = 3$ ) and enhances oxidation resistance by forming protective  $Al_2O_3$  layers. Additionally, Al tends to segregate to the surface under high temperatures, facilitating the formation of catalytically active sites.

Nickel is a key element with  $VEC = 10$ , forms the FCC phase, characterized by a dense atomic arrangement and, consequently, a high number of catalytic sites. In the ternary Ni-Co-Fe system, Ni significantly enhances catalytic activity and plays a pivotal role in CO oxidation reactions.

Other chemical elements serve as auxiliary components, enhancing the physicochemical properties of the HEA: cobalt improves the mechanical properties and is active in CO reactions; iron (Fe) stabilizes the mixed FCC+BCC phase and forms  $Fe_2O_3$  oxides that can act as active centers; copper increases the alloy's plasticity and exhibits a tendency for surface segregation; manganese enhances high-temperature stability and forms oxides that serve as catalytically active centers. All selected elements possess either BCC or FCC lattices, a critical factor in HEA formation.

Among numerous options, the following compositions were chosen: Al<sub>28</sub>Ni<sub>22</sub>Co<sub>17</sub>Fe<sub>15</sub>Cu<sub>10</sub>Mn<sub>8</sub>, Al<sub>32</sub>Mn<sub>23</sub>Ni<sub>17</sub>Fe<sub>8</sub>Cu<sub>8</sub>Co<sub>12</sub>, Al<sub>32</sub>Ni<sub>15</sub>Co<sub>13</sub>Mn<sub>15</sub>Fe<sub>10</sub>Cu<sub>15</sub>, and Al<sub>20</sub>Ni<sub>20</sub>Co<sub>20</sub>Fe<sub>20</sub>Cu<sub>20</sub>. Analytical review of existing literature suggests that equiatomic compositions, such as Al<sub>20</sub>Ni<sub>20</sub>Co<sub>20</sub>Fe<sub>20</sub>Cu<sub>20</sub>, are optimal for HEA formation. However, challenges arise in synthesizing this material via thermochemical pressing due to Al high reactivity, which initiates reactions and requires a higher concentration. Thus, the Al<sub>20</sub>Ni<sub>20</sub>Co<sub>20</sub>Fe<sub>20</sub>Cu<sub>20</sub> configuration was taken as a reference for ideal conditions.

Although the chemical composition remains constant, the molar ratio plays a crucial role in selecting the optimal system. Among the four variants, the system must meet specific physicochemical and thermodynamic criteria:  $\Delta S_{mix}$  should range from 13.4 to 22 J/(mol·K), the phase should be FCC, BCC, or a combination thereof, and the alloy must exhibit stability and capability for CO oxidation and potentially CO<sub>2</sub> hydrogenation.

The selected systems share similar characteristics, but each warrants individual evaluation to justify the choice. The Al<sub>20</sub>Ni<sub>20</sub>Co<sub>20</sub>Fe<sub>20</sub>Cu<sub>20</sub> system is equiatomic, a significant advantage for HEA formation, but its near-minimum  $\Delta S_{mix}$  value makes it less favorable. The Al<sub>28</sub>Ni<sub>22</sub>Co<sub>17</sub>Fe<sub>15</sub>Cu<sub>10</sub>Mn<sub>8</sub> system, with high Ni (22 %) and Co (17 %) content, plays a critical role in oxidation and hydrogenation reactions. Its  $T \cdot \Delta S_{mix}$  value indicates good high-temperature stability, essential for catalytic applications. With a VEC of 7.43, it suggests a mix of FCC and BCC phases, ensuring a high diversity of catalytic sites. Additionally, its  $\Delta S_{mix}$  is sufficiently high for successful HEA formation. The Al<sub>32</sub>Mn<sub>23</sub>Ni<sub>17</sub>Fe<sub>8</sub>Cu<sub>8</sub>Co<sub>12</sub> system has an adequate  $\Delta S_{mix}$ , but its key elements, Al and Mn, are more relevant for volatile organic compound (VOC) oxidation than CO catalysis. The Al<sub>32</sub>Ni<sub>15</sub>Co<sub>13</sub>Mn<sub>15</sub>Fe<sub>10</sub>Cu<sub>15</sub> system exhibits the highest  $\Delta S_{mix}$  among the selected variants, but its key elements and application variations indicate it is unsuitable for the intended purposes. Detailed modeling results are presented in Tabl. 2.

Table 2. Comparative characteristics of key HEA parameters for determining the optimal composition

Alloy configuration	$\Delta S_{mix}$	$T \cdot \Delta S_{mix}$	VEC	Phase	Key elements	Using
Al <sub>20</sub> Ni <sub>20</sub> Co <sub>20</sub> Fe <sub>20</sub> Cu <sub>20</sub>	13,38	21,40	8,2	FCC	Ni, Co, Cu	Hydration CO <sub>2</sub> , oxidation CO
Al <sub>28</sub> Ni <sub>22</sub> Co <sub>17</sub> Fe <sub>15</sub> Cu <sub>10</sub> Mn <sub>8</sub>	14,20	22,71	7,43	FCC+B CC	Ni, Co, Cu	Hydration CO <sub>2</sub> , oxidation CO
Al <sub>32</sub> Mn <sub>23</sub> Ni <sub>17</sub> Fe <sub>8</sub> Cu <sub>8</sub> Co 12	13,82	22,11	6,87	BCC або FCC+B CC	Al, Mn	Oxidation VOC, com- bustion
Al <sub>32</sub> Ni <sub>15</sub> Co <sub>13</sub> Mn <sub>15</sub> Fe <sub>10</sub> Cu <sub>15</sub>	14,25	22,79	7,13	FCC+B CC	Cu, Ni, Mn	CO <sub>2</sub> hydro- genation, re- forming

After conducting a series of mathematical calculations and analyzing literature sources related to the development of high-entropy alloys, it was hypothesized that the most advantageous and suitable system for our purposes has the configuration Al<sub>28</sub>Ni<sub>22</sub>Co<sub>17</sub>Fe<sub>15</sub>Cu<sub>10</sub>Mn<sub>8</sub>. Detailed results are presented in Tabl. 3.

Table 3. Table of Gibbs energy change dependence on temperature for the Al<sub>28</sub>Ni<sub>22</sub>Co<sub>17</sub>Fe<sub>15</sub>Cu<sub>10</sub>Mn<sub>8</sub> alloy

Temperature, K°	$\Delta H_{mix}$ , kJ/mol	$\Delta S_{mix}$ , kJ/mol	$\Delta G_{mix}$ , kJ/mol	$T \Delta S_{mix}$ kJ/mol
400	-14,59	14,20	-20.27	5.67
600			-23.11	8.51
800			-25.95	11.35
1000			-28.79	14.19
1200			-31.63	17.03
1400			-34.47	19.87
1600			-37.31	22.71

High *Ni* and *Co* content ensures active catalytic sites, while *Cu* (10 %) may segregate to the surface, enhancing efficiency. High-temperature stability is confirmed by a  $T \cdot \Delta S_{mix}$  value exceeding 20 kJ/mol at 1400 K and above.

Fig. 1 illustrates that the Al<sub>28</sub>Ni<sub>22</sub>Co<sub>17</sub>Fe<sub>15</sub>Cu<sub>10</sub>Mn<sub>8</sub> alloy is thermodynamically stable across a wide temperature range; however, varying *Al* content may destabilize the phase at lower temperatures. This underscores the importance of optimizing the composition for specific operating conditions, particularly for high-temperature applications such as catalysis. Regions where the surface properties change abruptly may indicate temperatures or compositions at which phase transitions (e.g., FCC → BCC) could occur, necessitating further analysis using diffraction data.

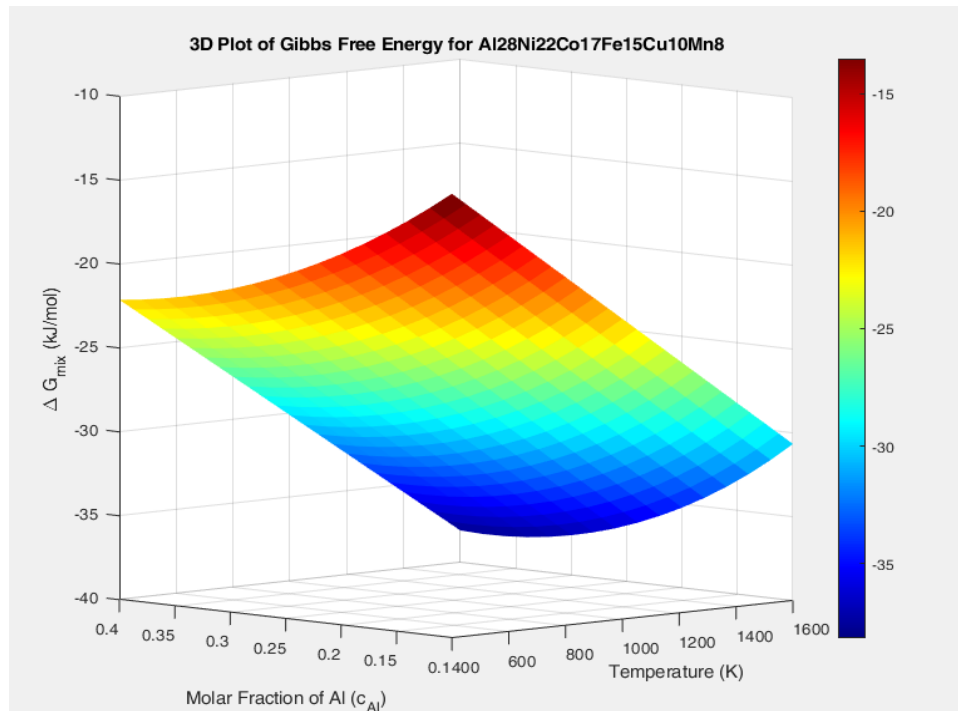


Fig. 1.  $\Delta G_{mix}$  as a function of temperature *T* and the molar fraction of one of the elements

Fig. 2 illustrates that a VEC  $\approx 7.43$  indicates a boundary between FCC and BCC phases (FCC predominates at VEC  $> 8$ , BCC at VEC  $< 6.87$ ). At VEC = 7.43, the alloy may form either FCC or BCC phases, depending on temperature. The graph demonstrates that at low temperatures (400 K),  $\Delta G_{mix}$  is less negative ( $\approx -7$  kJ/mol), which may favor the formation of the BCC phase, whereas at 1600 K ( $\Delta G_{mix} \approx -15$  kJ/mol), the FCC phase becomes more stable due to the entropic contribution.

For modeling the crystal lattice of Al<sub>28</sub>Ni<sub>22</sub>Co<sub>17</sub>Fe<sub>15</sub>Cu<sub>10</sub>Mn<sub>8</sub>, the VESTA visualization software was employed, significantly aiding in the depiction of the structure. However, to simulate the placement of atoms within BCC and FCC crystal lattices, a custom Python script was developed, which, within the framework of these lattice concepts, randomly positioned the atoms of the elements. The powder diffraction pattern enables confirmation of the crystal lattice by comparing peak positions with expected  $2\theta$  values.

Fig. 3 illustrates the three-dimensional FCC crystal lattice model and the powder diffraction pattern of Al<sub>28</sub>Ni<sub>22</sub>Co<sub>17</sub>Fe<sub>15</sub>Cu<sub>10</sub>Mn<sub>8</sub>. Peaks characteristic of FCC (e.g., (111), (200)) confirm that the model accurately reproduces the FCC phase. The shift in peaks due to the supercell ( $2\theta \approx 10^\circ$  instead of  $42.6^\circ$ ) is expected, as the supercell lattice parameter ( $a = 7.2$  Å) is twice that of the unit cell ( $a = 3.6$  Å). The FCC phase, as demonstrated by thermodynamic calculations, is stable at VEC  $\approx 7.43$ , consistent with the model. This aids in predicting whether the FCC phase will remain dominant under varying conditions (temperature, pressure).

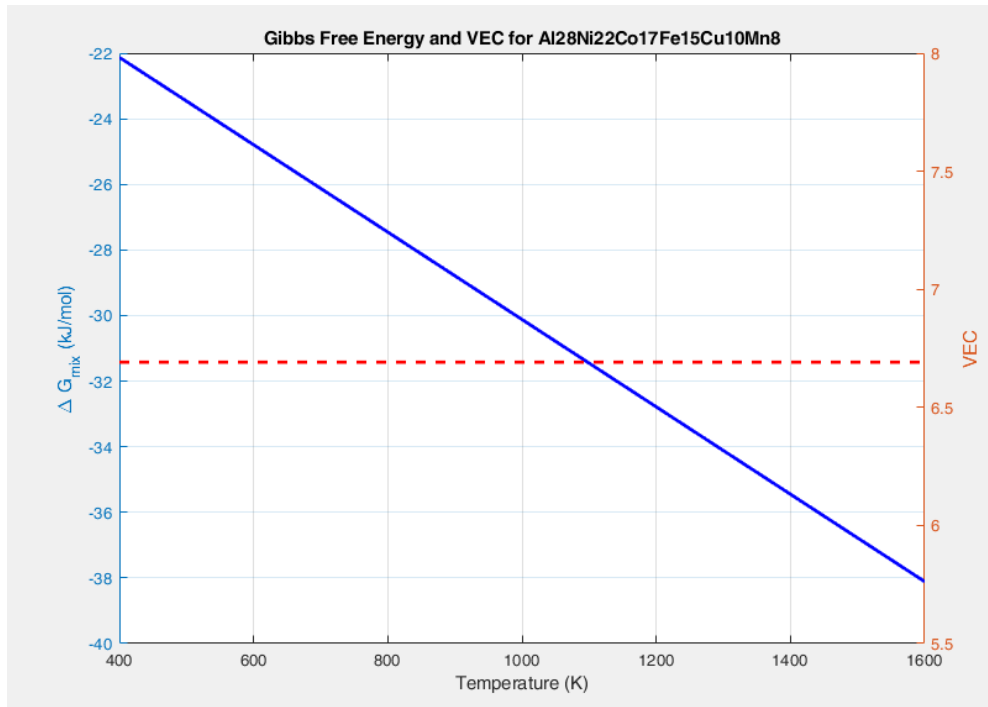


Fig. 2.  $\Delta G_{\text{mix}}$  and VEC as a function of temperature

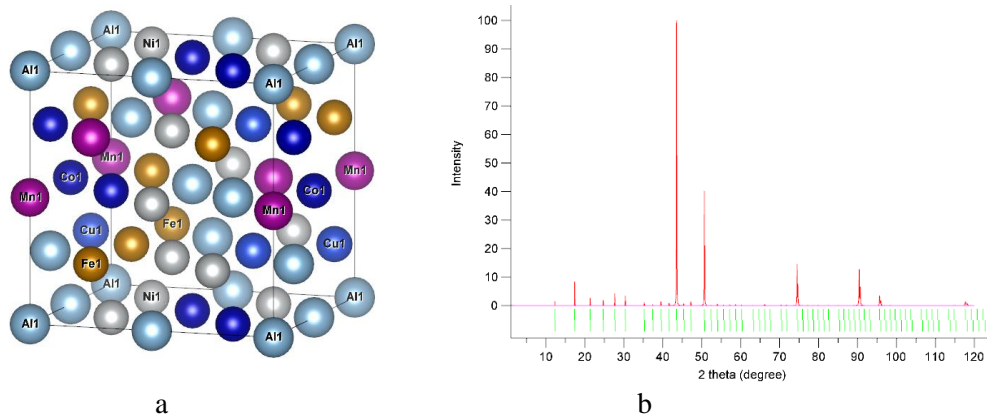


Fig. 3. FCC three-dimensional crystal lattice model(a) and powder diffraction plot(b)

The three-dimensional BCC crystal lattice model and the powder diffraction pattern of  $\text{Al}_{28}\text{Ni}_{22}\text{Co}_{17}\text{Fe}_{15}\text{Cu}_{10}\text{Mn}_8$  are depicted in Fig. 4. Peaks characteristic of BCC (e.g., (110), (200)) confirm that the model accurately reproduces the BCC phase. The shift in peaks due to the supercell ( $2\theta \approx 10^\circ$  instead of  $44.7^\circ$ ) is expected, as the supercell lattice parameters ( $a = 5.74 \text{ \AA}$ ,  $c = 11.48 \text{ \AA}$ ) are larger than those of the unit cell ( $a = 2.87 \text{ \AA}$ ). The BCC phase, as indicated by thermodynamic calculations, is plausible at  $\text{VEC} \approx 7.43$ , which aligns with the model.

The diffraction pattern confirms a highly crystalline structure for the  $\text{Al}_{28}\text{Ni}_{22}\text{Co}_{17}\text{Fe}_{15}\text{Cu}_{10}\text{Mn}_8$  HEA, with the dominant peak at  $2\theta \approx 90^\circ$  corresponding to the (440) plane, consistent with a Heusler-like cubic lattice similar to  $\text{Cu}_2\text{MnAl}$ . The narrow peaks and low background underscore excellent material quality, aligning with thermodynamic predictions of phase stability at  $\text{VEC} \approx 7.43$ , which supports a mix of FCC and BCC phases. The presence of weaker peaks at lower angles (e.g.,  $2\theta \approx 30^\circ$ ) suggests possible minor impurities or secondary phases, such as oxides or residual elemental

phases, which warrant further investigation. To validate the phase composition, comparison with JCPDS database entries for  $\text{Cu}_2\text{MnAl}$  and experimental compositional analysis (e.g., EDS) is recommended. The diffraction data reinforces the alloy's potential for high-temperature catalytic applications, but optimization of synthesis conditions may be needed to minimize impurities and ensure phase purity.

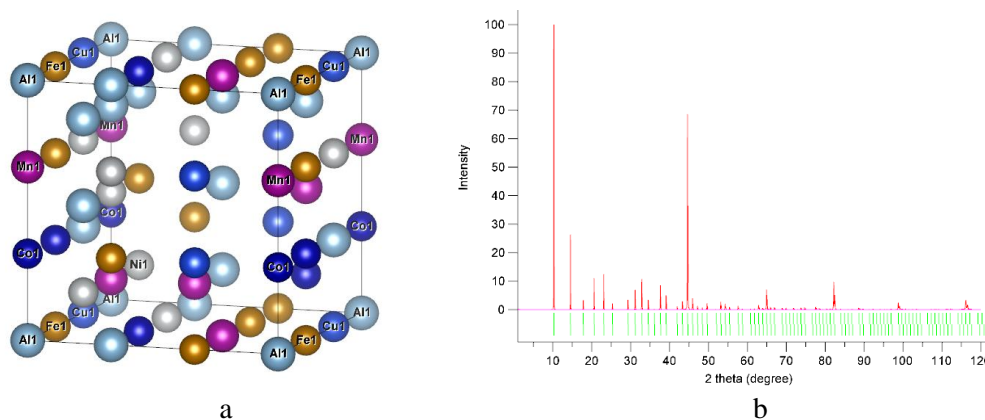


Fig. 4. BCC three-dimensional crystal lattice model powder diffraction plot

### Conclusions

This study elucidates the thermodynamic and structural attributes of the high-entropy alloy (HEA)  $\text{Al}_{28}\text{Ni}_{22}\text{Co}_{17}\text{Fe}_{15}\text{Cu}_{10}\text{Mn}_8$ , underscoring its potential as a robust catalytic material for thermochemical applications. Through meticulous mathematical modeling and literature analysis, the alloy's composition was optimized, revealing a high configurational entropy ( $\Delta S_{\text{mix}}$  within 13.4–22 J/(mol·K)) and favorable thermodynamic stability, as evidenced by  $\Delta G_{\text{mix}}$  values ranging from  $-7$  kJ/mol at 400 K to  $-15$  kJ/mol at 1600 K. The valence electron concentration ( $\text{VEC} \approx 7.43$ ) supports a dual FCC and BCC phase structure, enhancing catalytic site diversity, with high  $\text{Ni}$  and  $\text{Co}$  content driving efficacy in  $\text{CO}$  oxidation. Powder diffraction patterns, modeled using VESTA and custom Python scripts, confirmed the presence of FCC and BCC phases, though minor peaks suggest potential impurities warranting further investigation. These findings position HEAs as a transformative alternative to conventional catalysts, leveraging compositional flexibility to achieve superior resilience. Future research should prioritize experimental validation of phase purity via techniques like EDS and JCPDS database comparisons, alongside optimization of synthesis methods, such as thermochemical pressing, to mitigate  $\text{Al}$  reactivity. Additionally, integrating computational tools, including machine learning, could accelerate the design of tailored HEA compositions, broadening their impact across catalysis, aerospace, and energy sectors.

### References

- [1] Hongdong, L., Yi, H., Zhao, H., & iH. (2020). Fast site-to-site electron transfer of high-entropy alloy nanocatalyst driving redox electrocatalysis. *Nature Communications*, 11, 5196. <https://doi.org/10.1038/s41467-020-19277-9>
- [2] Dhakar, S., Sharma, A., Katiyar, N. K., & iH. (2023). Utilization of structural high entropy alloy for  $\text{CO}$  oxidation to  $\text{CO}_2$ . *Inorganic Chemistry Communications*, 158 (Частина 1), 111492. <https://doi.org/10.1016/j.inoche.2023.111492>
- [3] Mori, K., Hashimoto, N., Kamiuchi, N., & iH. (2021). Hydrogen spillover-driven synthesis of high-entropy alloy nanoparticles as a robust catalyst for  $\text{CO}_2$  hydrogenation. *Nature Communications*, 12, 4180. <https://doi.org/10.1038/s41467-021-24228-z>



- [4] Odetola, P. I., Babalola, B. J., Afolabi, A. E., & ін. (2024). Exploring high entropy alloys: A review on thermodynamic design and computational modeling strategies for advanced materials applications. *Heliyon*, 10(22), e39660. <https://doi.org/10.1016/j.heliyon.2024.e39660>
- [5] Minnuo Gas. (2024). *Coke oven gas purification*. [https://minnuogas.com/air\\_separation\\_plant/coke-oven-gas-purification/](https://minnuogas.com/air_separation_plant/coke-oven-gas-purification/)
- [6] Qiu, H.-J., Fang, G., Wen, Y., & ін. (2019). Nanoporous high-entropy alloys for highly stable and efficient catalysts. *Journal of Materials Chemistry A*, 7(11), 10338–10346. <https://doi.org/10.1039/C9TA00505F>
- [7] Sereda, B. P., Bielokon, K. V., Bielokon, Yu. O., & others. (2018). Model of the mechanism of catalytic reactions of carbon monoxide glycolysis. Bulletin of the National University "Lviv Polytechnic". Series: Chemistry, Technologies of Substances and Their Applications, (1(38)), 129–137. [https://doi.org/10.31319/2519-8106.1\(38\)2018.129017](https://doi.org/10.31319/2519-8106.1(38)2018.129017)
- [8] Yue, X., Shuhui, L., Yayang, Q., & ін. (2020). High-entropy alloys as a platform for catalysis: Progress, challenges, and opportunities. *ACS Catalysis*, 10(17), 9738–9768. <https://doi.org/10.1021/acscatal.0c03617>
- [9] Sun, Y., & Dai, S. (2021). High-entropy materials for catalysis: A new frontier. *Science Advances*, 7(20), eabg1600. <https://doi.org/10.1126/sciadv.abg1600>

### Список використаної літератури

1. Hongdong L., Yi H., Zhao H. et al. Fast site-to-site electron transfer of high-entropy alloy nanocatalyst driving redox electrocatalysis. *Nature Communications*. 2020. Vol. 11. Article 5196. DOI: 10.1038/s41467-020-19277-9.
2. Dhakar S., Sharma A., Katiyar N. K. et al. Utilization of structural high entropy alloy for CO oxidation to CO<sub>2</sub>. *Inorganic Chemistry Communications*. 2023. Vol. 158, part 1. Article 111492. DOI: 10.1016/j.inoche.2023.111492.
3. Mori K., Hashimoto N., Kamiuchi N. et al. Hydrogen spillover-driven synthesis of high-entropy alloy nanoparticles as a robust catalyst for CO<sub>2</sub> hydrogenation. *Nature Communications*. 2021. Vol. 12. Article 4180. DOI: 10.1038/s41467-021-24228-z.
4. Odetola P. I., Babalola B. J., Afolabi A. E. et al. Exploring high entropy alloys: A review on thermodynamic design and computational modeling strategies for advanced materials applications. *Heliyon*. 2024. Vol. 10, iss. 22. Article e39660. DOI:10.1016/j.heliyon.2024.e39660.
5. Coke oven gas purification. Minnuo Gas. 2024. URL: [https://minnuogas.com/air\\_separation\\_plant/coke-oven-gas-purification/](https://minnuogas.com/air_separation_plant/coke-oven-gas-purification/)
6. Qiu H.-J., Fang G., Wen Y. et al. Nanoporous high-entropy alloys for highly stable and efficient catalysts. *Journal of Materials Chemistry A*. 2019. Vol. 7, iss. 11. P. 10338–10346. DOI: 10.1039/C9TA00505F.
7. Середя Б. П., Белокоп К. В., Белокоп Ю. О., Кругляк І. В. Модель механізму каталітичних реакцій гліколізу оксиду вуглецю. Вісник Національного університету "Львівська політехніка". Серія: Хімія, технології речовин та їх застосування. 2018. № 1(38). С. 129–137. DOI: 10.31319/2519-8106.1(38)2018.129017.
8. Yue Xin, Shuhui Li, Yayang Qian et al. High-entropy alloys as a platform for catalysis: progress, challenges, and opportunities. *ACS Catalysis*. 2020. Vol. 10, iss. 17. P. 9738–9768. DOI: 10.1021/acscatal.0c03617.
9. Sun Y., Dai S. High-entropy materials for catalysis: A new frontier. *Science Advances*. 2021. Vol. 7, iss. 20. Article eabg1600. DOI: 10.1126/sciadv.abg1600.

Надійшла до редколегії 28.03.2025